



OPEN ACCESS

EDITED BY
Guanglong Sheng,
Yangtze University, China

REVIEWED BY
Dongjun Song,
Lanzhou University, China
Shuncun Zhang,
Northwest Institute of Eco-
Environment and Resources (CAS),
China

*CORRESPONDENCE
Lu Zhou,
zhoulu9@126.com

SPECIALTY SECTION
This article was submitted to Economic
Geology,
a section of the journal
Frontiers in Earth Science

RECEIVED 24 May 2022
ACCEPTED 16 September 2022
PUBLISHED 09 January 2023

CITATION
Wang X, Zhou L, Wu Y, Li S, Gu Y and Li X
(2023), Factors controlling spatial
distribution of complex lithology in
transitional shale strata: Implications
from logging and 3D seismic data, Shan-
2 Lower Sub-member, Eastern
Ordos Basin.
Front. Earth Sci. 10:951524.
doi: 10.3389/feart.2022.951524

COPYRIGHT
© 2023 Wang, Zhou, Wu, Li, Gu and Li.
This is an open-access article
distributed under the terms of the
[Creative Commons Attribution License
\(CC BY\)](https://creativecommons.org/licenses/by/4.0/). The use, distribution or
reproduction in other forums is
permitted, provided the original
author(s) and the copyright owner(s) are
credited and that the original
publication in this journal is cited, in
accordance with accepted academic
practice. No use, distribution or
reproduction is permitted which does
not comply with these terms.

Factors controlling spatial distribution of complex lithology in transitional shale strata: Implications from logging and 3D seismic data, Shan-2 Lower Sub-member, Eastern Ordos Basin

Xuxu Wang¹, Lu Zhou^{1,2*}, Yong Wu^{1,3}, Shuxin Li⁴, Yifan Gu¹ and Xingtao Li⁴

¹School of Geoscience and Technology, Southwest Petroleum University, Chengdu, China, ²State Key Laboratory of Oil and Gas Reservoir and Exploration, Southwest Petroleum University, Chengdu, China, ³Natural Gas Geology Key Laboratory of Sichuan Province, Southwest Petroleum University, Chengdu, China, ⁴PetroChina Coalbed Methane Company, Beijing, China

The Shanxi Formation Shan-2 Lower Sub-member transitional shale in the eastern Ordos Basin is characterized by high total organic carbon value, wide distribution, and large single-layer/cumulative thickness; it is the key target interval for transitional shale gas exploration. Based on drilling, logging, 3D seismic, and natural energy spectrum data, this study discusses the spatial distribution and controlling factors of complex lithology in the transitional shale stratum. Using the multi-lithological eigenvalue method, the lithologic differential distribution characteristics of the Shan-2 Lower Sub-member were identified through seismic attribute analysis and post-stack seismic parameter inversion. On this basis, the controlling factors of lithology spatial difference distribution are revealed by paleogeomorphology restoration, the sedimentary environmental indicator characteristics of shale, and seismic facies division. The results indicate that the lithology distribution of transitional shale strata in the Shan-2 Lower Sub-member is significantly different, and the geomorphological pattern of interjacent depressions and highlands lays a foundation for the formation of the sedimentary system. The environmental and energy differences of paleo-sedimentary water form a sedimentary environment with frequent facies transitions, which controls the distribution of sediments. Th/U and Th/K ratios, which indicate redox conditions and sedimentary water energy during the early sedimentary stage of the Shan-2 Lower Sub-member, show that the geomorphic uplift area is characterized by a high-energy transitional environment of mainly developed sandstone and silty mudstone, while the depression is relatively low-energy under a brackish water reduction environment, mainly composed of both dark and carbonaceous shale. During the late sedimentary stage of the Shan-2 Lower Sub-member, when geomorphic control was weakened, it presented a shallow-water, high-energy, and oxidized transitional environment, with a lithology dominated by

the complex interbedding of fine-grained sandstone, silty shale, shale, carbonaceous shale, and coal seam. Therefore, it is inferred that the Shan-2 Lower Sub-member may have developed as a barrier island-lagoon sedimentary model. The early depositional period was dominated by barrier island-lagoon-tidal flat depositional combination, thence the sedimentary environment gradually evolved into a tidal flat-swamp environment.

KEYWORDS

Eastern Ordos basin, Shan-2 Lower Sub-member, transitional facies, lithologic spatial distribution, sedimentary model

1 Introduction

In recent years, Chinese geologists have discovered a number of marine-continental transitional shale-gas enrichment areas in the Permian of the eastern Ordos Basin and the Carboniferous-Permian of the southern Sichuan Basin. To date, the proven geological resources have amounted to $19.79 \times 10^{12} \text{ m}^3$, accounting for 25% of total shale-gas resources in China; the recoverable resources are $3.48 \times 10^{12} \text{ m}^3$, indicating a huge exploration potential (Dong et al., 2012, 2016; Zou et al., 2016; Guo et al., 2018; Kuang et al., 2020). At present, marine shales are dominant in known shale oil and gas reservoirs and have been efficiently developed on a large-scale in the United States, Canada, and China (Zou et al., 2015; Qiu and Zou, 2020; Guan et al., 2021). However, globally, the exploration and exploitation of marine-continental transitional shale gas is still in its infancy (Liang Q. S. et al., 2018). In contrast to marine shale developed in deep-water shelf environments, marine-continental transitional shales are usually deposited in the epicontinental sea-lagoon-delta transitional environments under conditions of marine regression (Liu et al., 2018; Luo et al., 2018; Zhang et al., 2018; Xiao et al., 2019). Therefore, such transitional shales are not only defined by marked variation in the sedimentary cycles of continental shale layers but also by the occurrence of sedimentary microfacies and their sedimentary responses to sea-level fluctuations (Zhang, 2015). Marine-continental transitional shales are characterized by numerous thin producing layers, irregular vertical and spatial distributions, high organic carbon contents, medium thermal maturity, and good gas-bearing properties (Wang et al., 2011; Yan et al., 2013; Wu et al., 2021; Zhang et al., 2022). Currently, the geological study of transitional facies is still at an early stage, and the formation environment, reservoir characteristics, and enrichment conditions are unclear—restricting the large-scale production and development of transitional shale gas.

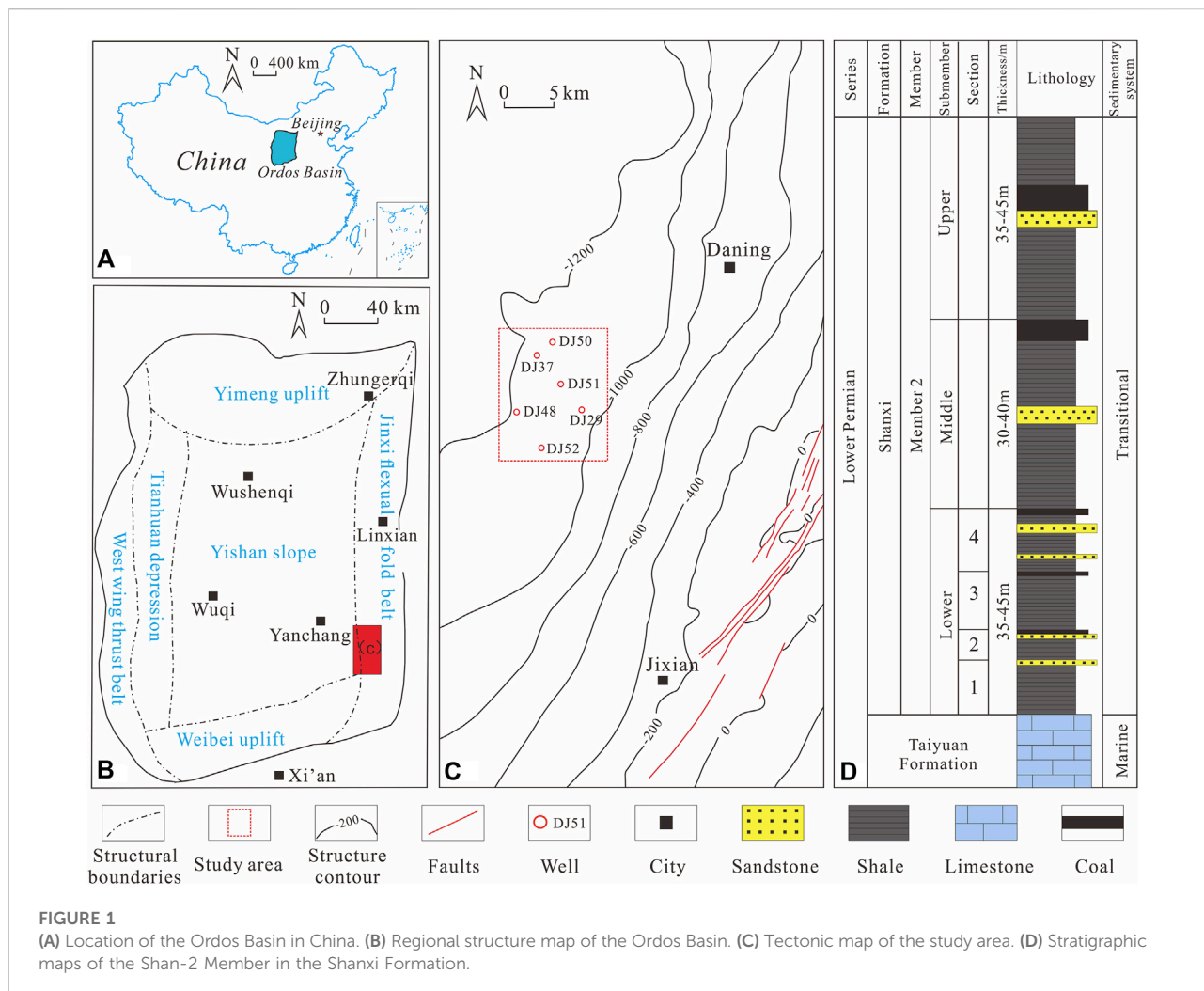
The Permian Shanxi Formation in the eastern Ordos Basin is a typical marine-continental transitional sedimentary system (Dong et al., 2021) with a large cumulative thickness of shale. However, compared to marine shale, marine-continental transitional shale has particularities and complexities with respect to aspects such as depositional range, water depth, and sediment distribution; its sedimentary environment changes more frequently and its lithologic assemblage becomes more complex. Previous studies concentrated on the evaluation of

different lithofacies (Wu et al., 2021), macroscopic reservoir characteristics (Wei et al., 2020), microscopic pore structure, and gas content (Sun et al., 2017; Qiu et al., 2021), which have explained the heterogeneity of the vertical variation and reservoir characteristics of transitional shale. However, the plane distribution characteristics of transitional shale remain unclear. The poor understanding of the spatial distribution of complex lithology in transitional facies, as well as controversy over the sedimentary model of transitional shale, has led to an unclear understanding of the development characteristics and distribution law of transitional shale, thus hampering the prediction of shale-gas sweet spots.

Previous studies have shown that paleo-geomorphic characteristics, changes in the sedimentary environment, facies, and sedimentary rates are closely related to the spatial distribution and heterogeneity of sediments, and that shale-reservoir characteristics are also controlled by them (Zhu et al., 2003; Ursula and Gregory, 2012; Konitzer et al., 2014; Chen et al., 2015; Hou et al., 2018). However, the spatial distribution and controlling factors of complex lithology in transitional facies remain unclear. If the spatial distribution of lithology and its controlling factors can be clarified, then identifying shale-gas sweet spots should be more effective and accurate, combined with the evaluation parameters of shale reservoirs. High-quality seismic data have been collected in a pilot test area of the south-eastern margin of the Ordos Basin, which have provided the basis for this study. This study combines the latest drilling, logging, and 3D seismic data, based on the identification of complex lithology, the controlling factors of lithologic spatial difference distribution revealed by paleogeomorphology restoration, natural energy spectrum analysis, and seismic facies division. The sedimentary characteristics of the transitional shale stratum in this area are further understood, and the sedimentary model types are further discussed, providing the theoretical basis for identifying the development location of organic-rich shale.

2 Geological setting

The Ordos Basin developed in the North China Craton and has an area of $370,000 \text{ km}^2$ (Figures 1A,B). The Ordos Basin can



be divided into six secondary structural units: the Yimeng Uplift, the Western Fold-Thrust Belt, the Tianhuan Depression, the Shenbei Slope, the Jinxi Flexural Fold Belt, and the Weibei Uplift (Yang et al., 2005, Figure 1B). As the main sedimentary area of the North China Platform, it formed, during the Late Carboniferous period, a sedimentary pattern bounded by the central paleo-uplift which was deposited in the east and west sea areas. During the Early Permian Taiyuan Formation period, the east and west seas overlapped the central paleo-uplift, forming a unified epicontinental sea deposition. During the Early Permian Shanxi Formation period, affected by the Hercynian tectonic movement, the northern margin of the North China Platform was rapidly uplifted, the north-south difference manifested, and seawater gradually withdrew from the basin from both its eastern and western sides. At this time, the provenance from the north was rapidly filled, and alluvial plains, deltas, shallow lakes, and lagoons were developed from north to south, forming a sedimentary pattern from land to sea (Tian, 2016). It was a transitional sedimentary stage between marine and continental

environments against a background of an epeiric platform. The sedimentary system of shore-shallow sea, lagoon, and tide-controlled delta was developed. During the Late Permian Shiqianfeng Formation period, the seawater completely withdrew, and the Ordos Basin evolved from an early offshore lake basin to an inland lake basin (Li et al., 2021; Wu et al., 2021).

The study area is located south of the Jinxi flexure fold belt in the eastern Ordos Basin (Figures 1B,C). Under the influence of the Caledonian tectonic movement, the Middle Ordovician strata were uplifted and denuded, and the Late Ordovician and the Early Carboniferous strata were missing. Multistage transitional sedimentary cycles were formed on the unconformity surface of the Middle Ordovician and many sets of high-quality transitional shale strata were deposited, including the Upper Carboniferous Benxi Formation, the Early Permian Taiyuan Formation, and the Shanxi Formation (Wang et al., 2011; Yan et al., 2013). The Early Permian Shanxi Formation is divided into the Shan 1 and Shan 2 Members; the cumulative thickness of the Shan-2 Member shale is 21.4–92.3 m, with an average thickness of 41.2 m (Luo,

2013; Kuang et al., 2020). The shale in the Shan-2 Lower Sub-member is stably distributed, with coal and thin sandstone interlayers, and complex and diverse lithologic combinations. The average total organic carbon (TOC) is as high as 7.97%, indicating great shale gas resource potential. In addition, Wells DJ51 and JP1H have achieved high production during the gas test of the transitional shale at the bottom of the Shan-2 Lower Sub-member, demonstrating good development prospects. According to the characteristics of down-hole lithologic assemblage and the distribution of organic-rich shale, the Shan-2 Lower Sub-member is further divided into four sections (Figure 1D).

3 Methodology

Seven wells were drilled through the Lower Permian Shanxi Formation in the study area, from which complete logging data were obtained. Among them, three outcrops and continuous coring wells were selected for observation and description. The three-dimensional seismic data cover 100 km² in the study area, with an effective bandwidth of 15–60 Hz and a main frequency of 35 Hz. The available seismic data were collected, processed, and provided by PetroChina Coalbed Methane Co., Ltd.

3.1 Sedimentological characterization

Field investigations were conducted from the eastern Ordos Basin, including the Chengjiazhuang outcrop in Liulin, the Taitou outcrop in Xiangning, and the Jushuihe outcrop in Hancheng. We observed the sedimentary structures and lithology combination of the Shanxi Formation and noted them by camera for further analysis. In the study area, Well DJ51 provided a continuous core of the Shan-2 Lower Sub-member. Core observation has identified different lithologies, including coal, fine-grained sandstone, siltstone, shale, and carbonaceous shale, and recorded the lithology combination of different sections. Observation and description of the sedimentary structure and lithologic combination emphasize frequent sedimentary environment changes and the complex characteristics of lithologic combination in marine-continental transitional facies.

3.2 Seismic identification method of complex lithology

3.2.1 Seismic attribute analysis

Seismic amplitude information is widely used in the lithologic interpretation of seismic data. The amplitude or energy characteristics of reflected waves are commonly used dynamic attributes in lithologic interpretation. The attributes are extracted by amplitude characteristic analysis, which often

reflects the spatial variation of the formation medium (wave impedance, strata thickness, petrographic composition, fluid, and lithologic combination) of the target layer, and can be used to track stratigraphic characteristics and identify lithologic changes (Lu and Wang, 2009). The Lower Permian Shanxi Formation is a typical marine-continental transitional depositional system, characterized by the complex interbedding of shales, sandstones, and coals (Figure 2); its spatial variation is rapid, with different lithologic combinations causing the difference in seismic reflection characteristics. The Shan-2 Lower Sub-member shows the variation of waveform characteristics in the seismic profile (Figure 3): lateral changes of the seismic wave amplitude and waveform (peak and trough), poor continuity, and local polarity reversal. On this basis, combined with the seismic amplitude attributes, the change of seismic amplitude in vertical and horizontal directions is analyzed, which can be used to indicate the spatial variation of complex lithologic combinations in the Shan-2 Lower Sub-member.

3.2.2 Spatial distribution prediction of complex lithology

The complexity of the lithological assemblage of the marine-continental transitional facies in the study area, including its marked and commonly abrupt spatial and vertical variations, presents challenges to the interpretation of seismic data. In this study, we characterized the complexity of the lithology and the spatial distribution of organic-rich shale using the multi-lithological eigenvalue method.

Lithological variation in standard wells (DJ51) was constrained using drill-core observations, logging data, and analysis and testing data. The logging response characteristics of down-well lithologies were established and the extremum point of the discrete random sequence for each logging parameter curve was selected using extreme value theory (Figure 4), as given in Eq. 1:

$$P_i = \begin{cases} P_i \geq P_{(i+1)} \& P_i \geq P_{(i-1)}; \text{Maximum} \\ P_i \leq P_{(i+1)} \& P_i \leq P_{(i-1)}; \text{Minimum} \end{cases} \quad (1)$$

In Eq. 1, P_i represents the extreme point, $P_{(i+1)}$ represents the point behind the extreme point, and $P_{(i-1)}$ represents the point before the extreme point.

The lithology corresponding to the extremum point P_i (h , litho, V_p , GR , ...) is the eigenvalue of a particular lithology. This point also has associated values of multiple petrophysical parameters. The values of parameters corresponding to the extreme point were analyzed by multi-parameter petrophysical intersection, allowing cross-plots of logging response parameters for different lithologies to be generated (GR -Velocity). By standardizing other wells, similar features to those of standard wells were identified, allowing logging response parameters to be used to characterize lithological complexity. Of these parameters, the

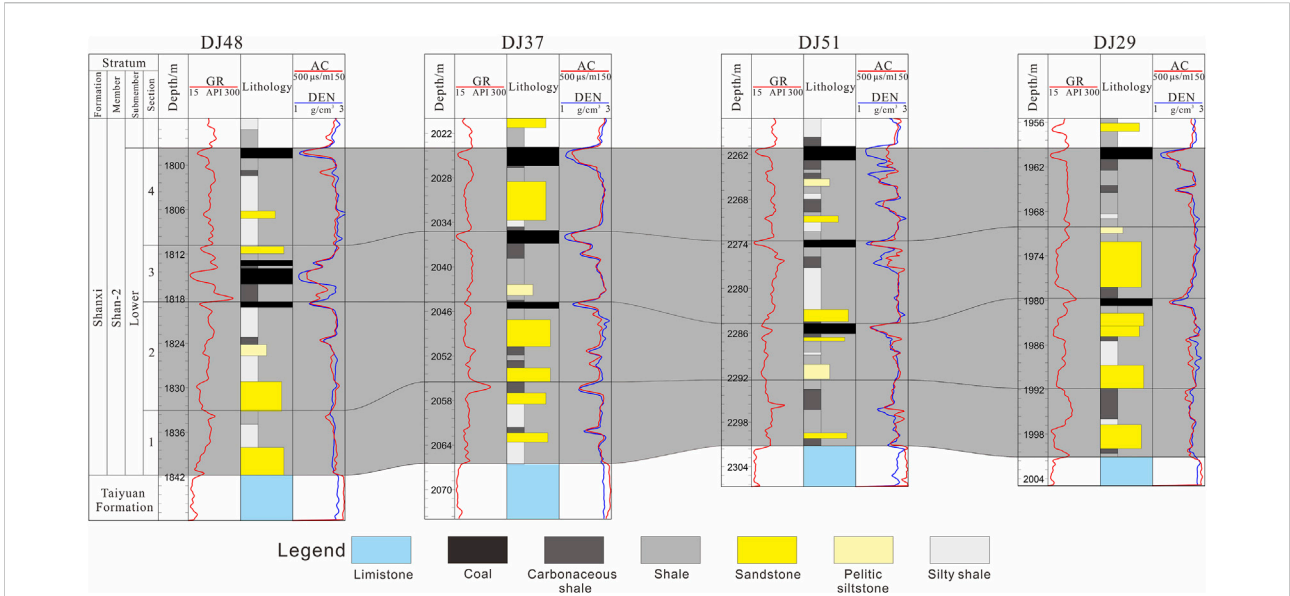


FIGURE 2
Stratigraphic correlation of connecting wells of the Shan-2 Lower Sub-member in the eastern Ordos Basin.

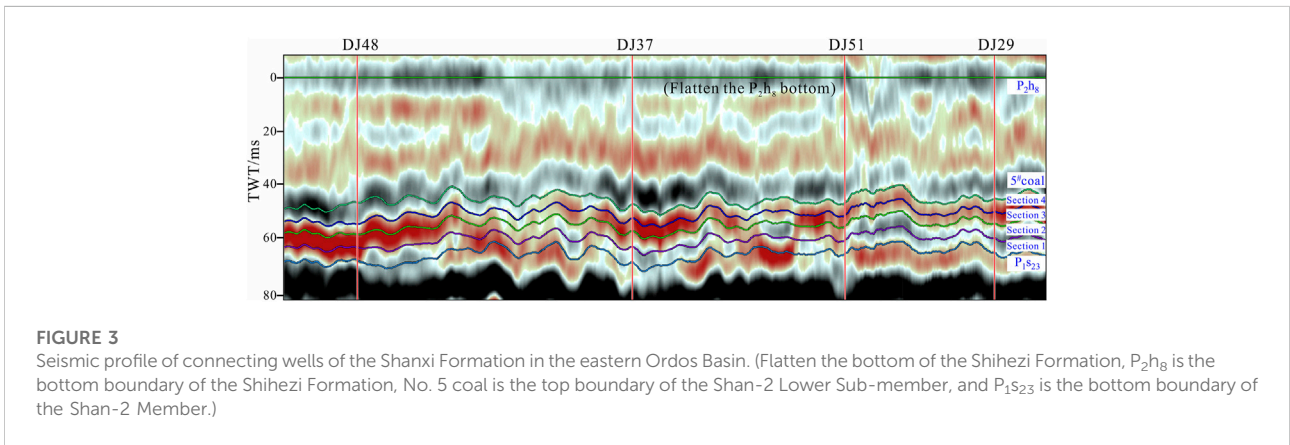


FIGURE 3
Seismic profile of connecting wells of the Shanxi Formation in the eastern Ordos Basin. (Flatten the bottom of the Shihezi Formation, P_{2h8} is the bottom boundary of the Shihezi Formation, No. 5 coal is the top boundary of the Shan-2 Lower Sub-member, and P_{1s23} is the bottom boundary of the Shan-2 Member.)

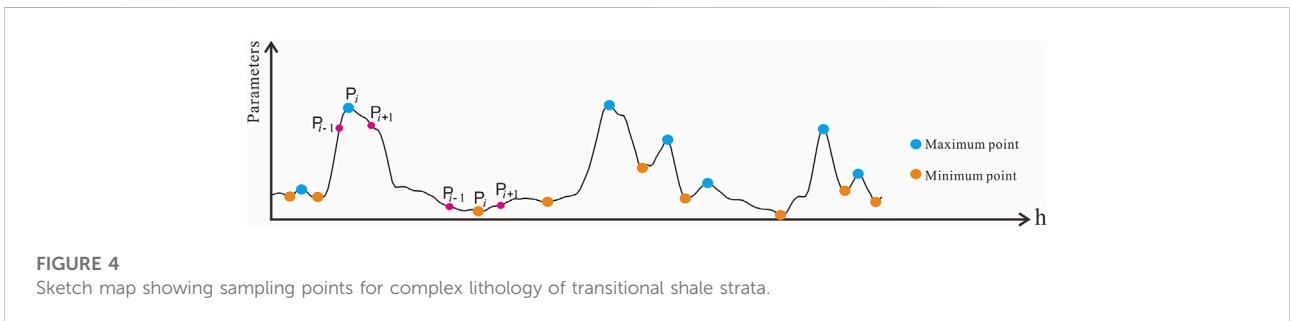
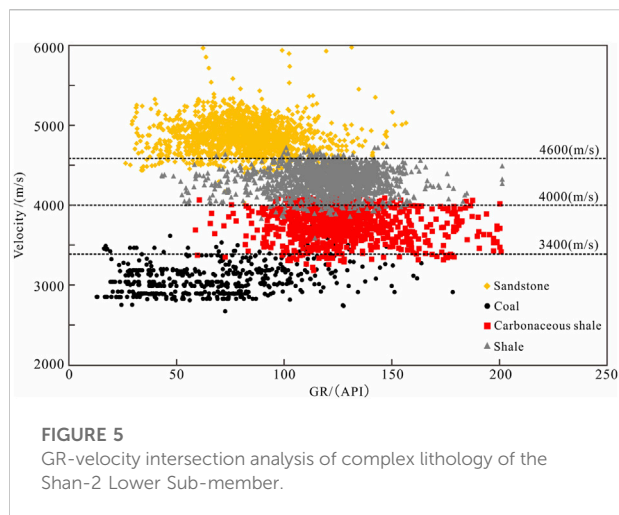


FIGURE 4
Sketch map showing sampling points for complex lithology of transitional shale strata.



seismic velocity of sandstone is $> 4,600$ m/s, that of mud shale is $4,000$ – $4,600$ m/s, that of carbonaceous shale is $3,400$ – $4,000$ m/s, and that of coal seams is $< 3,400$ m/s (Figure 5). By using inversion of seismic velocity parameters, the velocity volume of inversion was transformed into the lithology volume using the velocity differences between lithologies so as to realize the effective identification of complex lithology in marine-continental transitional shale strata. The inversion modelled results correspond well with the observed lithological variation established from drill-cores.

3.3 Restoration of paleogeomorphology

The impression method was the main method used for restoring paleogeomorphology in this study. The theoretical basis of the impression method is filling-leveling up (Jin et al., 2017). In this method, the base level of the upper part of the target horizon for paleogeomorphologic restoration is first identified, and the No. 5 coal seam at the top of the Shan-2 Lower Sub-member is distributed uniformly throughout the study area; it can be used as a datum for paleogeomorphologic restoration in the study area (Figure 2). Based on multi-lithology identification, the porosity conversion model was used to reconstruct the depositional thicknesses of different lithological strata. The mirror relationship between residual paleogeomorphology and overlying strata is then fully utilized and semi-quantitative restoration of paleogeomorphology is realized by the thickness of overlying strata.

3.4 Seismic facies analysis

Seismic facies is a seismic feature formed by the sedimentary environment (Sheriff, 1982; Xu and Haq, 2022). The types of seismic facies are distinguished by the differences in reflected wave characteristics (amplitude, frequency, and continuity) on the

seismic profile, which are then interpreted as corresponding sedimentary facies types to reflect the change characteristics of the sedimentary environment. Seismic waveform clustering analysis as an effective seismic facies analysis method mainly identifies the differential changes of amplitude, frequency, and phase of the seismic waveform by neural network and pattern recognition, and divides different seismic facies types (Jiang et al., 2012; Ding et al., 2020). In this study, the waveform clustering methods were preferentially selected to analyze the seismic facies characteristics.

4 Results

4.1 Sedimentological characteristics

In the transitional zone of north-south provenance in the eastern Ordos Basin, seawater during the sedimentary period of the Shanxi Formation gradually withdrew from the basin from both its eastern and western sides, forming a typical sedimentary environment of transitional facies (Kuang et al., 2020; Wu et al., 2021). According to the down-hole lithology characteristics and core observation results (Figures 2, 6), the Shanxi Formation Shan-2 Member is characterized by complex lithologic combinations: ① frequent thin interbeds of sandstone and silty shale (Figure 6A); ② interbedding of sandstone, silty shale, shale, and coal (Figures 6B,C); and ③ frequent interbedding of gray shale and thin sandstone (Figure 6D).

The lithology of Section 1 has obvious lateral changes, with well DJ48 being mainly composed of sandstone and silty shale. Well DJ37 is characterized by sand-mud interbedding. Well DJ29 is characterized by sandstone and gray-black carbonaceous shale. Well DJ51 is dominated by gray-black shale and carbonaceous shale, with the shale at the bottom containing marine bioclastics such as crinoids and brachiopods (Figure 6G). In Section 2, the sandy sediments increase, being mainly developed sandstone, gray shale, and silty shale. The shale is characterized by horizontal bedding, with a thin black coal seam at the top (Figure 6H). In Section 3, Well DJ48 comprises the coal seam and carbonaceous shale. Wells DJ37 and DJ51 are dominated by shale and silty shale, with plant debris contained in shale (Figure 6F). The thick sandstone is developed in Well DJ29. Section 4 comprises the gray shale, silty shale, with thin sand layers, and the No. 5 coal seam is present at the top. The shale is characterized by horizontal bedding (Figure 6E). The spatial variation of lithology reflects rapid changes of the transitional environment under sea level changes, forming the complex and diverse lithologic assemblages in the study area.

4.2 Lithological spatial distribution

4.2.1 Seismic attributes analysis

The variation of the amplitude attributes in the Shan-2 Lower Sub-member indicates the spatial difference in the distribution of complex lithologic combinations in transitional facies. The seismic

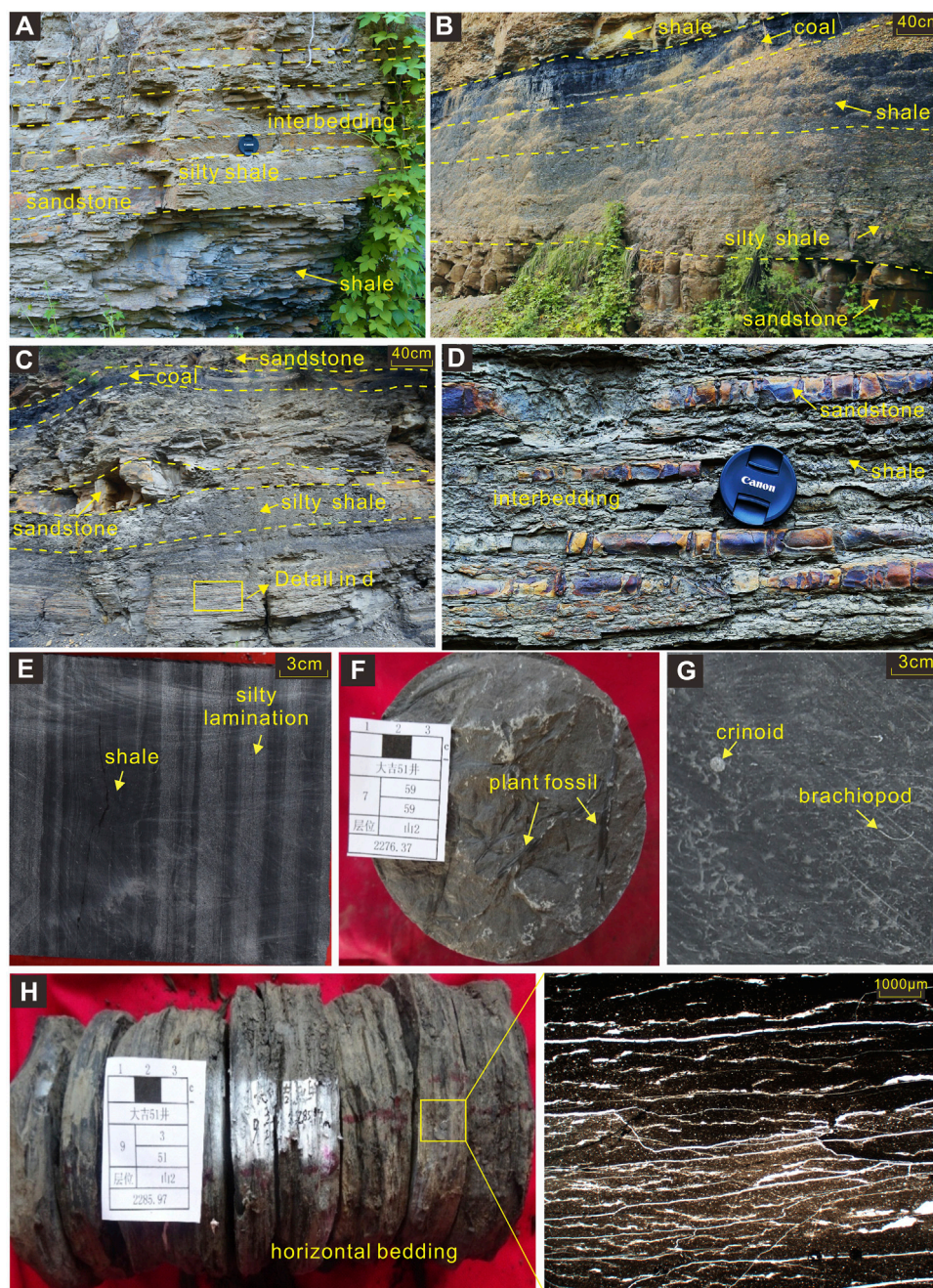


FIGURE 6

Sedimentary characteristics for Shanxi Formation Shan-2 Member from outcrops and cores in the eastern Ordos Basin. (A) Frequent thin interbeds of sandstone and silty shale, with the lower part being shale, Shan-2 Member, Taitou outcrop. (B,C) Interbedding of shale, coal, sandy shale, and sandstone, Shan-2 Member, Taitou outcrop. (D) Frequent interbedding of shale and thin sandstone, Shan-2 Member, Taitou outcrop. (E) Shale and silty lamination interbedding and horizontal bedding, Well DJ3-4, 2,123.2 m, Section 4. (F) Gray silty shale containing plant debris, Well DJ51, 2,276.37 m, Section 3. (G) Gray-black shale containing marine bioclasts including crinoids and brachiopods, Well DJ51, 2,294.89 m, Section 1. (H) Gray-black shale and horizontal bedding, Well DJ51, 2,285.97 m, Section 2).

amplitude plane characteristics were combined with the lithologic combination of each section in the well. In Section 1, the amplitude value of $-3,998\sim-747$ represents the combination of sandstone and

silty shale, mainly distributed in the Well DJ48 area, the amplitude value between -747 and 879 represents sand-mud interbedded deposition, and the amplitude value of $879\sim 4,131$ is the

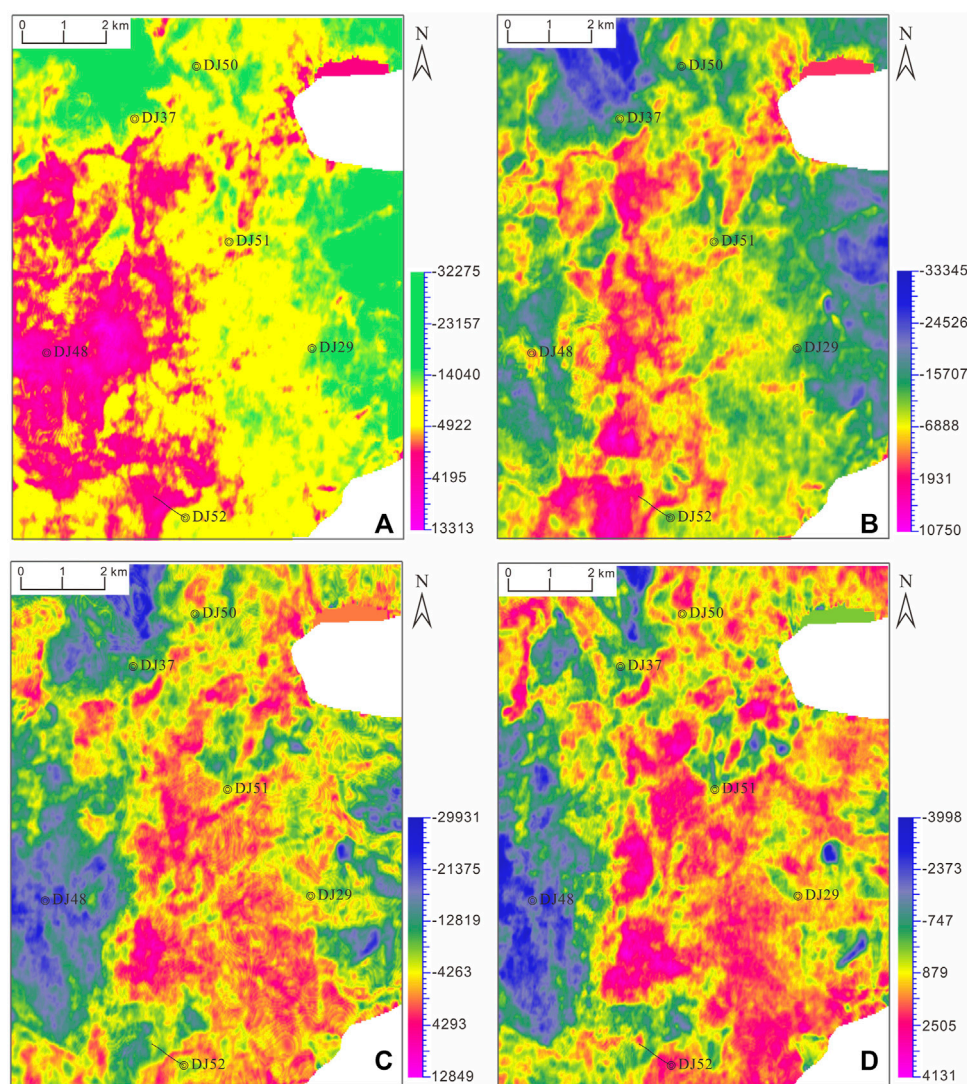


FIGURE 7

Minimum amplitude attribute plane distribution of each section in the Shan-2 Lower Sub-member in the eastern Ordos Basin: (A) Section 4; (B) Section 3; (C) Section 2; (D) Section 1.

combination of gray-black shale and carbonaceous shale, mainly distributed in the middle of the study area (Figure 7D). The amplitude value of $-4,263$ – $12,849$ in Section 2 represents gray shale and silty shale, and the amplitude value between $-7,000$ and $-4,263$ correspond to shale and carbonaceous shale, both of which are distributed evenly in the middle of the study area, while the amplitude value of -29931 – $-7,000$ corresponds to the combination of sandstone and shale, which are mainly distributed in the area of Well DJ48, north of Well DJ37, and east of Well DJ29 (Figure 7C). The amplitude value of $-6,888$ – $10,750$ and -15707 – -33345 in Section 3 represents the combination of shale and carbonaceous shale. The amplitude

value between -15707 and $-6,888$ corresponds to sandstone, which is mainly distributed in the south-west of Well DJ29 (Figure 7B). The amplitude value of -32275 – $-4,922$ in Section 4 corresponds to the combination of shale, silty shale, and carbonaceous shale, while the amplitude value of $-4,922$ – $13,313$ corresponds to sandstone and silty shale deposition (Figure 7A). The results show that the spatial variation of amplitude can reflect the differential distribution of different lithologic combinations, which reflects the characteristics of rapid change of the sedimentary cycle of transitional facies and also identifies the rough distribution range of different lithologies.

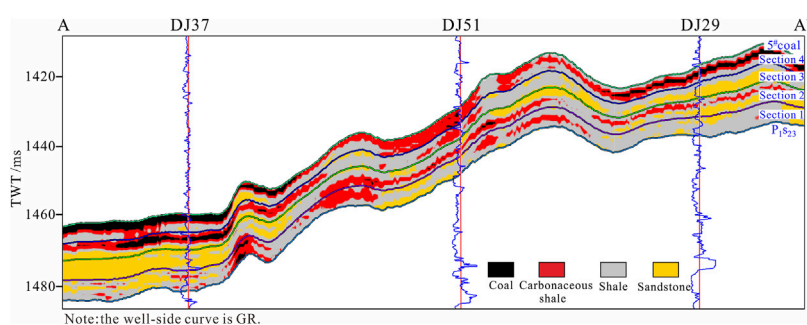


FIGURE 8

Lithologic inversion profile of the Shan-2 Lower Sub-member in the eastern Ordos Basin (see A–A' in Figure 9 for profile location).

4.2.2 Lithologic spatial difference distribution

The lithology changes frequently and the single layer thickness is thin in the Shan-2 Lower Sub-member of the Shanxi Formation. It is important to emphasize the spatial distribution of lithology in transitional facies for identifying sedimentary systems. On the premise of single-well lithology identification, the spatial distribution characteristics of each lithology in transitional shale strata are clarified by using the multi-lithologic eigenvalue value identification method.

According to the lithologic inversion profile, the lithologic distribution characteristics of each section are different. Section 1 is dominated by shale, with local thin sandstone and carbonaceous shale. Section 2 is mainly composed of sandstone, shale, and carbonaceous shale. Section 3 comprises the shale and carbonaceous shale in Wells DJ37–DJ51, with thin coal seams, while sandstone and shale are developed around Well DJ29. Section 4 is dominated by shale and carbonaceous shale, with the No. 5 coal seam at the top (Figure 8).

Based on the prediction of down-hole lithologic distribution, the plane prediction results of the lithology of each section can be extracted; the respective plane distribution characteristics of lithology are shown in Figure 9. Section 1 comprises mainly shale, sandstone, and carbonaceous shale. Sandstone is primarily distributed in the area of Wells DJ48–DJ52, while also being sporadically distributed in the eastern and northern portions of the study area. Carbonaceous shale is distributed in the middle of the study area, along an NW–SE direction (Figure 9D). Section 2 has developed sandstone and shale. The distribution range of sandstone is significantly greater than in Section 1, being distributed in flakes in the area of Wells DJ48, DJ29, and DJ37. The shale and silty shale are primarily distributed in the middle of the study area, and carbonaceous shale is distributed sporadically, with coal seam being developed near Well DJ52 (Figure 9C). Section 3 is mostly composed of sandstone, shale, and carbonaceous shale. The distribution range of sandstone is

significantly smaller than in Section 2, being mainly distributed south of Well DJ29 and sporadically distributed in the north. The distribution range of carbonaceous shale increases, mainly distributed in the area of Wells DJ52–DJ48–DJ37–DJ50, and the coal seams in this section gradually increase (Figure 9B). In Section 4, the distribution range of sandstone is further narrowed, being distributed near Well DJ52 and south of Well DJ37. The distribution of carbonaceous shale is mainly distributed in the northern area of Wells DJ29–DJ51–DJ50. The shale and silty shale are distributed in the middle of the study area, and in the area around Well DJ48 (Figure 9A). The lithology of the Shan-2 Lower Sub-member has obvious vertical and lateral differences and changes rapidly, reflecting the characteristics of the complex lithology combinations of transitional facies.

4.3 Paleogeomorphologic characteristics

Based on the lithologic spatial variation in the study area, the de-compaction correction impression method was used to restore the paleogeomorphology of the Shan-2 Lower Sub-member. Three geomorphological units were identified—highland, gentle slope, and depression—forming a geomorphological spatial pattern of “interjacent depressions and highlands” in the study area.

The paleogeomorphologic map after normalization of the stratum thickness is shown in Figure 10 to highlight the paleogeomorphology characteristics of the Shan-2 Lower Sub-member. In the early deposition stage of the Shan-2 Lower Sub-member, the area of Well DJ48, to the north of Well DJ37 and to the east of Well DJ29 show the uplift landforms, and the low landforms of depression distributed in the area of Wells DJ50–DJ51–DJ52 (Figure 10A). After the deposition of Sections 1 and 2, the geomorphic pattern is similar to the early deposition stage, and the paleogeomorphologic characteristics of low in the middle and high on both sides. However, the landform of the

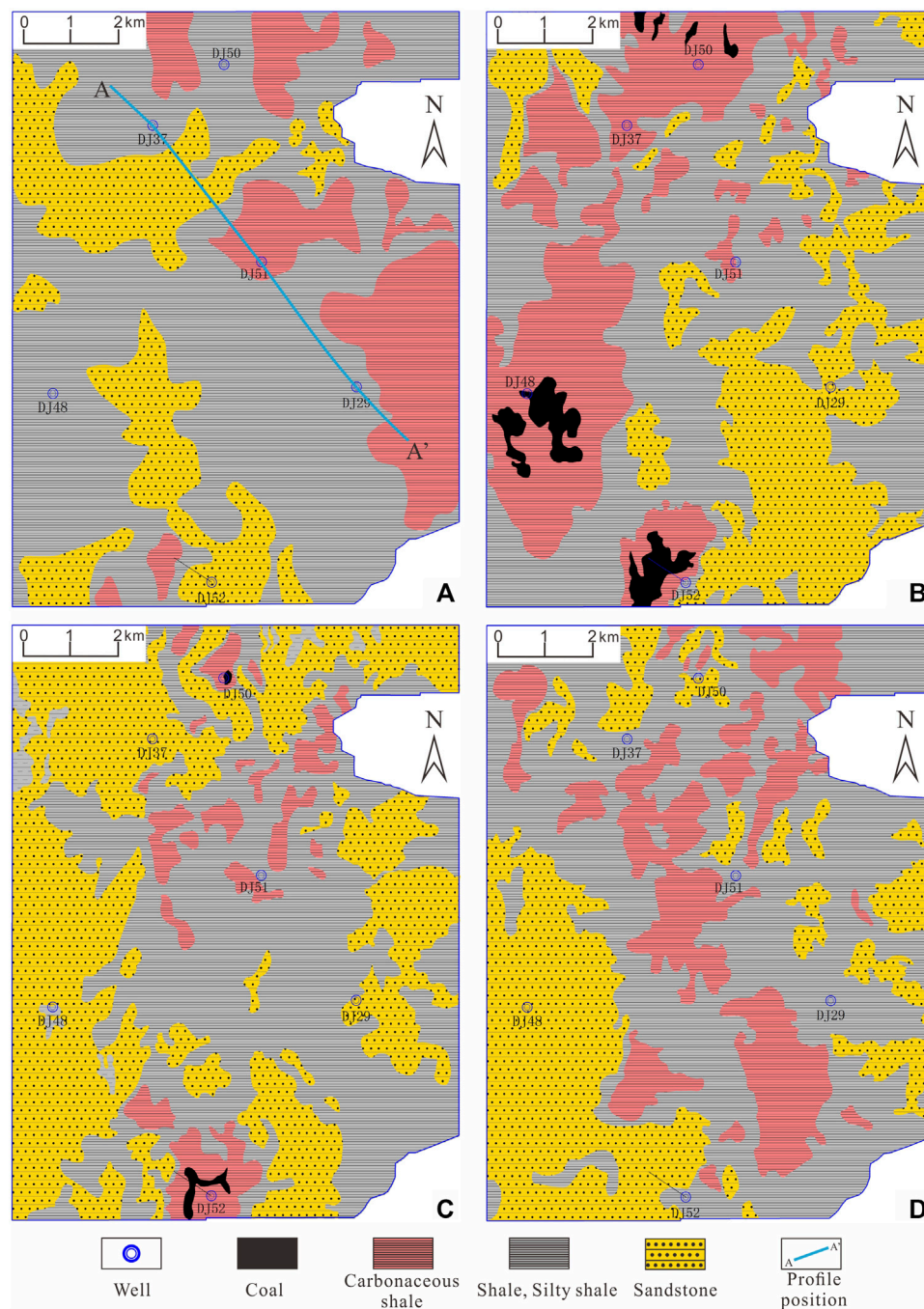


FIGURE 9

Lithologic plane distribution of each section in the Shan-2 Lower Sub-member in the eastern Ordos Basin. (A) Section 4; (B) Section 3; (C) Section 2; (D) Section 1.

study area became relatively gentle, and the slope area increased (Figure 10B). The paleogeomorphological units are classified with respect to compaction-corrected strata thickness (Table 1) (i.e., highlands, gentle slopes, and depressions), the distributions of which are shown in Figure 10.

4.4 Seismic facies characteristics

Based on the seismic facies identification technology of waveform clustering, the actual seismic traces in the Shan-2 Lower Sub-member are compared and analyzed, and the plane

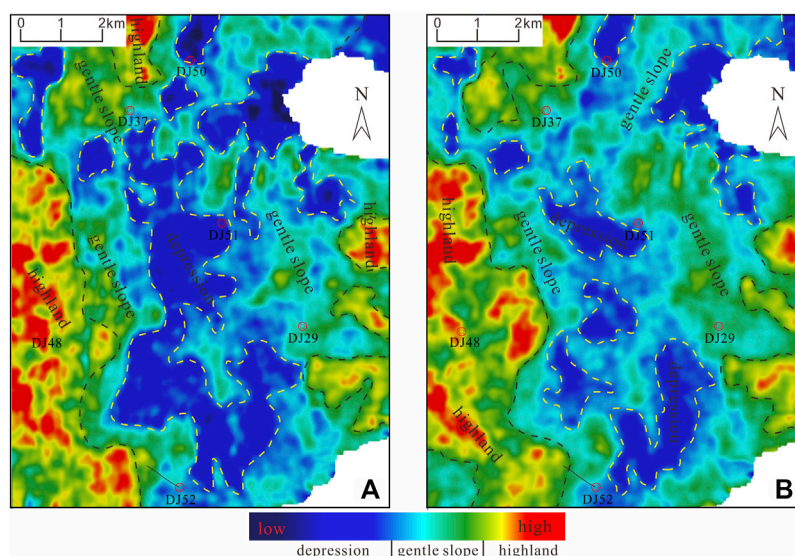


FIGURE 10
Sedimentary paleogeomorphologic maps of the Shan-2 Lower Sub-member restored using the residual thickness method during the initial stage of deposition (A) and the late stage of deposition (B).

TABLE 1 The characteristics of the paleogeomorphological units and the division standard in the early deposition stage of Shan-2 Lower Sub-member.

Geomorphological unit	Characterization	Division standard (impression thickness)	Typical wells
Highlands	Regions with the highest elevations of paleogeomorphology, their impression thickness is usually thin	Impression thickness < 85 m	DJ48
Gentle slopes	Areas with slower slopes	85 m < impression thickness < 100 m	DJ37, DJ29
Depressions	Areas with the lowest of paleogeomorphology, their impression thickness is thick	100 m < impression thickness	DJ50, DJ51

distribution characteristics of seismic facies in the study area are clarified. Section 1 can be divided into five types of seismic facies (Figure 11D). The blue area shows low frequency and medium amplitude wave-trough reflection; the light-blue area shows low frequency and strong amplitude wave-trough reflection; the yellow area shows low frequency and weak amplitude wave-peak reflection; the red area shows medium frequency and medium-weak amplitude wave-peak reflection; the green area shows medium frequency and medium amplitude wave-peak reflection (Table 1).

Section 2 can be divided into five types of seismic facies (Figure 11C), although its seismic waveform characteristics are different from Section 1. The blue area shows low frequency and strong amplitude wave-trough reflection; the light-blue area shows low frequency and weak amplitude wave-trough

reflection; the green area shows medium frequency and medium amplitude wave-peak reflection; the yellow area shows medium-low frequency and weak amplitude wave-peak reflection; the red area shows medium frequency and medium amplitude wave-peak reflection (Figure 11C; Table 2).

Four types of seismic facies can be identified in Section 3. In Figure 11B, the blue area is dominated by low frequency and weak amplitude wave-trough reflection; the yellow area shows medium-low frequency and medium-strong amplitude wave-trough reflection; the red area is dominated by medium frequency and weak amplitude wave-trough reflection; the green area is dominated by medium frequency and medium-strong amplitude wave-trough reflection (Figure 11B; Table 2).

Three types of seismic facies can be identified in Section 4 (Figure 11A). The yellow area is of medium frequency and

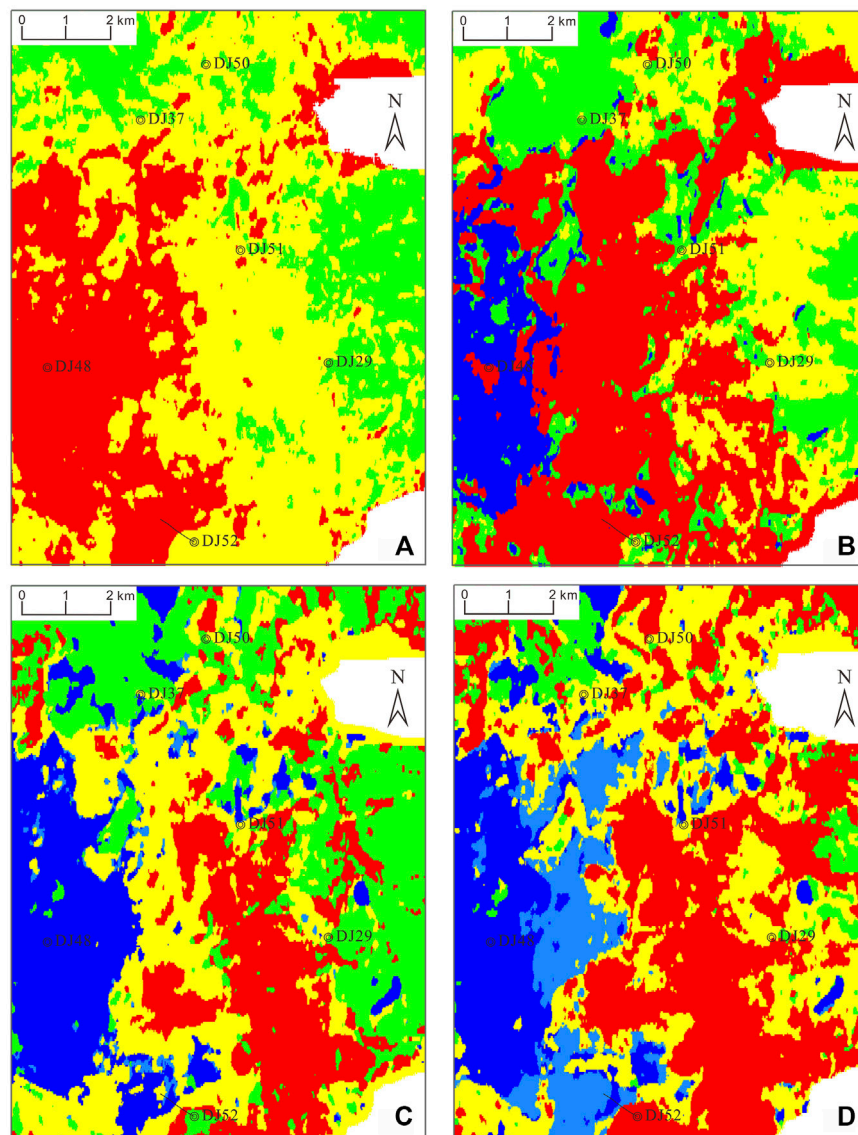


FIGURE 11

Seismic facies plane distribution of each section in the Shan-2 Lower Sub-member in the eastern Ordos Basin: (A) Section 4; (B) Section 3; (C) Section 2; (D) Section 1.






medium-weak amplitude wave-trough reflection; the red area is of medium-low frequency and medium-weak amplitude wave-peak reflection; the green area is of medium frequency and medium-strong amplitude wave-trough reflection (Figure 11A; Table 2).

5 Discussion

The sedimentary cycle of marine–continental transitional facies strata changes rapidly, with the sedimentary environment

playing an important role in controlling the formation of shale strata. The differential changes of the paleogeographic pattern and sedimentary environment further affect the differences of lithologic combinations (Zhang et al., 2015; Li et al., 2021; Wu et al., 2021). Performing paleogeomorphic restoration, gamma-ray spectrum analysis, and seismic facies analysis in the study area, as well as clarifying the controlling factors of the lithologic difference distribution of transitional shale strata will help deepen our understanding of the sedimentary system and laws in this area.

TABLE 2 Correspondence between seismic facies types and seismic reflection characteristics in the Shan-2 Lower Sub-member.

Section, Types	Section 1	Section 2	Section 3	Section 4
	Medium frequency, medium amplitude, wave-peak reflection	Medium frequency, medium amplitude, wave-peak reflection	Medium frequency, medium-strong amplitude, wave-trough reflection	Medium frequency, medium-strong amplitude, wave-trough reflection
	Medium frequency, medium-weak amplitude, wave-peak reflection	Medium frequency, medium amplitude, wave-peak reflection	Medium frequency, weak amplitude, wave-trough reflection	Medium-low frequency, medium-weak amplitude, wave-peak reflection
	Low frequency, weak amplitude, wave-peak reflection	Medium-low frequency, weak amplitude, wave-peak reflection	Medium-low frequency, medium-strong amplitude, wave-trough reflection	Medium frequency, medium-weak amplitude, wave-trough reflection
	Low frequency, strong amplitude, wave-trough reflection	Low frequency, weak amplitude, wave-trough reflection		
	Low frequency, medium amplitude, wave-trough reflection	Low frequency, strong amplitude, wave-trough reflection	Low frequency, weak amplitude, wave-trough reflection	

5.1 Paleogeomorphologic characteristics and its controlling effect

Paleogeomorphologic characteristics play an extremely important role in controlling the development and distribution of sedimentary systems, mainly affecting the type of sedimentary system and lithologic distribution characteristics by controlling the sediment dispersion system in the sedimentary basin (Meng and Ji, 2009; Liu et al., 2012).

At the initial stage of deposition of the Shan-2 Lower Sub-member (Sections 1 and 2), the difference between highlands and depressions in the study area is great (Figure 10A), resulting in the enhancement of hydrodynamic action near the highlands and forming a relatively high energy sedimentary environment. Barrier islands or sand ridges are formed in the geomorphic uplift area and sandstone is relatively developed. The water body is relatively deep in the depression, with mainly lagoon facies deposition, and comprises the dark shale and carbonaceous shale (Figures 9C,D). After the deposition of Sections 1 and 2, the landform of the study area became relatively gentle compared to the initial stage of deposition (Figure 10B) and the water body became relatively shallow. Carbonaceous shale and shale were widely deposited in the study area, thin coal seams were developed locally, and the distribution range of sandstone became significantly reduced (Figures 9A,B). Combined with the sedimentary background and lithologic characteristics of the study area, one can conclude that tidal flat-swamp facies deposits dominated during this period.

This result shows that the geomorphological pattern of interjacent depressions and highlands lays a foundation for the formation of the sedimentary system, which can affect the change of the sedimentary water in the study area and then control the sediment plane distribution of each section (Figures 9, 10).

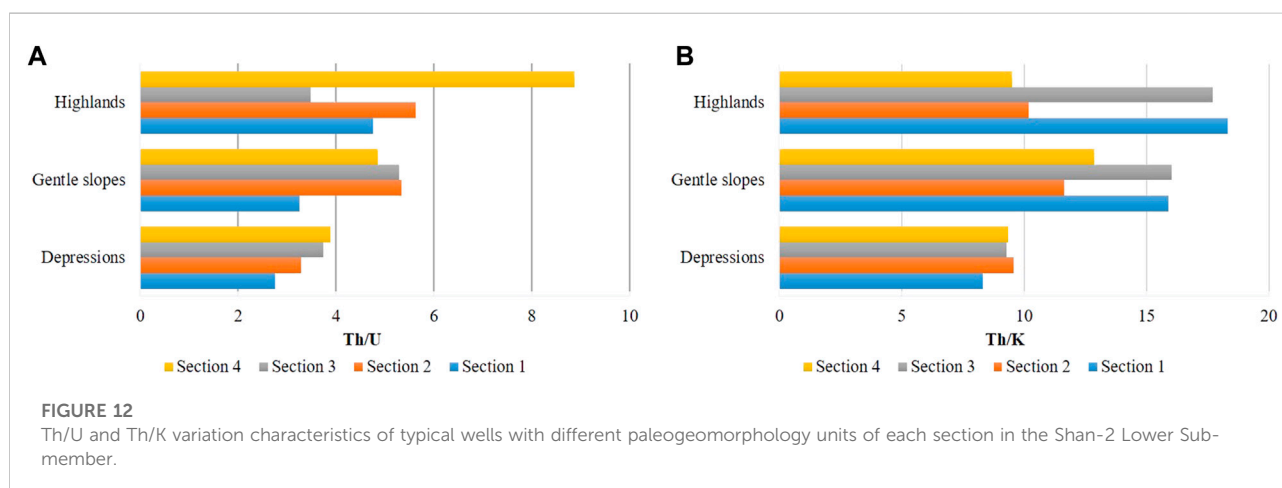
5.2 Characteristics of the natural energy spectrum and its significance

The Shan-2 lower sub-member in the study area comprises marine-continental transitional shale strata, which are controlled by the sedimentary environment. The natural energy spectrum logging curve can be used to determine the types and contents of different radioactive elements in the strata, the contents of elements, and Th/U and Th/K ratios which are of great significance in the study of sedimentary environments. Th/K mainly reflects the energy of sedimentary water: ratios of > 10 indicate a high-energy environment, 6–10 signify a sub-high-energy environment, and 3–6 indicate a low-energy environment. The Th/U ratio is used to determine the redox environment of shale. Ratios of Th/U > 7 signify a continental sedimentary environment of leaching and oxidation, 2–7 indicate a marine-continental transitional sedimentary environment, and < 2 signify a marine and strongly reducing sedimentary environment, with lithology of marine mudstone, carbonate rock, and phosphate (Feng et al., 2016; Zhao et al., 2016; Liang X. T. et al., 2018; He et al., 2019).

Three typical wells (DJ48, DJ37, and DJ51) in different geomorphic locations in the study area were selected for natural energy spectrum characteristics analysis. Table 3 lists the results obtained according to the corresponding relationship between natural energy spectrum characteristics and the sedimentary environment. In the highlands, the Th/U ratio in Sections 1, 2, and 3 is 2–7, and a Th/K ratio > 10 represents a high-energy, transitional environment. The Th/U ratio is 8.87 and the Th/K ratio is 9.51 in Section 4, representing a sub-high energy, oxidation environment. In the gentle slope area, Th/U is 2–7 and the Th/K ratio is > 10 , indicating that the slope area is dominated by a high-energy, transitional environment. In the depressions, the Th/U of Section 1 is 2.75 and the Th/K is 8.33, representing a sub-high-energy, weak reduction environment. The other three sections have Th/U

TABLE 3 Natural energy spectrum characteristics and sedimentary environment indications for typical wells in the Shan-2 Lower Sub-member.

Geomorphological unit	Typical well	Section	Th/U (avg.)	Th/K (avg.)	Sedimentary environment
Highlands	DJ48	1	4.76	18.32	High energy, transitional environment
		2	5.62	10.19	High energy, transitional environment
		3	3.48	17.72	High energy, transitional environment
		4	8.87	9.51	Sub-high energy, oxidized continental environment
Gentle slopes	DJ37	1	3.25	15.91	High energy, transitional environment
		2	5.33	11.63	High energy, transitional environment
		3	5.29	16.03	High energy, transitional environment
		4	4.85	12.87	High energy, transitional environment
Depressions	DJ51	1	2.75	8.33	Sub-high energy, weak reduction environment
		2	3.29	9.58	Sub-high energy, transitional environment
		3	3.74	9.29	Sub-high energy, transitional environment
		4	3.89	9.36	Sub-high energy, transitional environment



ratios of 2–7 and Th/K ratios of 6–10, representing a sub-high-energy, transitional environment.

This result shows that the Shan-2 Lower Sub-member was mainly deposited in a high-energy and sub-high-energy, transitional environment. The variation characteristics of the Th/U ratio show that the reducibility gradually weakens from the depressions to the highlands, from Sections 1 to 4. The Th/K ratio indicates that the hydrodynamic force is strong in the highlands and slope area, the depression is weak, and the energy of each section of the water body changes rapidly in a vertical direction (Figure 12). The environmental and energy differences of paleo-sedimentary water form a sedimentary environment with frequent facies transitions, which controls the distribution of sediments.

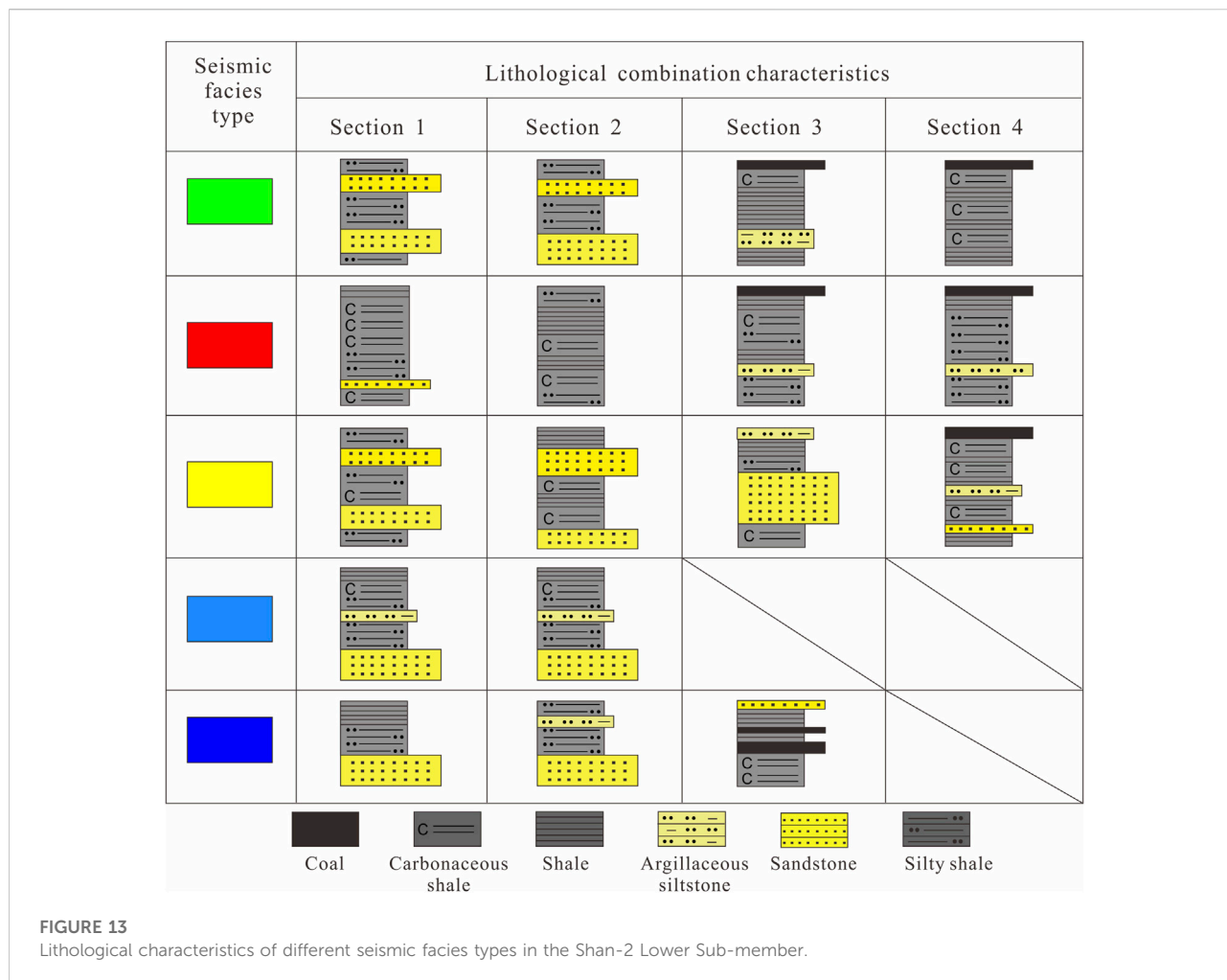
5.3 Seismic facies analysis

The sedimentary cycle of marine-continental transitional facies changes rapidly and the lithologic combination is

controlled by sedimentary microfacies (Zhang, 2015). In this study, the variations in seismic facies were used to analyze the change of the sedimentary environment in the Shan-2 Lower Sub-member. Based on the characteristics of paleogeomorphology and lithology assemblage, the types of sedimentary microfacies are analyzed, clarifying the corresponding relationship between sedimentary microfacies and lithologic spatial distribution.

The seismic facies types and lithologic assemblages of Sections 1 and 2 are similar. The blue and light-blue areas comprise the sandstone, silty shale and the shale, presented as positive rhythm characteristics and representing a barrier flat or sand ridge environment. The yellow and green areas comprise frequent interbeds of silty shale and sandstone, representing a tidal flat environment with frequent changes in energy. The red area comprises the gray-black shale and carbonaceous shale, and the shale contains marine bioclastics such as crinoids and brachiopods (Figure 6G), reflecting a lagoon or bay environment (Figures 11, 13).

In Section 3, the blue area comprises frequent interbeds of carbonaceous shale, thin coal seam, and shale, representing a



swamp environment. The yellow area comprises sandstone and shale, with the sandstone thickness increasing, reflecting increased terrigenous debris inflow and representing a delta front environment. The red and green areas comprise the silty shale, argillaceous siltstone, shale, and thin coal seam. Coal represents swamp, while silty shale and shale represent tidal flat (Figures 11, 13).

In Section 4, the yellow area comprises the carbonaceous shale, thin sandstone, and thin coal seam, representing a tidal flat-swamp environment. The red area comprises the silty shale and thin coal seam, with increased sandy sediments reflecting a tidal flat environment. The green area comprises the carbonaceous shale, shale, and thin coal seam, representing a swamp environment (Figures 11, 13).

The characteristics of lithological assemblages in the study area are controlled by sedimentary microfacies. Different seismic facies types have different lithologic combinations, and the sedimentary environments formed by them are also different. The spatial difference distribution of lithological assemblages reflects the rapid changes of the transitional environment under

the sea level changes. Meanwhile, the same sedimentary unit may produce different types of seismic facies because the same lithologic assemblage is different in the aspects of wave impedance, petrographic composition, fluid characteristics, and sedimentary microfacies, resulting in a difference in seismic waveforms and different types of seismic facies. The different facies in the same period are obvious, reflecting the rapid change of sedimentary microfacies, which affects the spatial distribution of sediments and forms the complex lithologic assemblage characteristics in this area.

5.4 Sedimentary model of transitional shales

As a transitional zone between marine and continental environments, marine-continental transitional facies include delta, estuarine, lagoon, barrier island, and tidal flat facies (Boyd et al., 1992; Galloway, 1998; Zhu, 2008; Jiang, 2010; Boggs, 2012; Dong et al., 2021). Dong et al. (2021), by

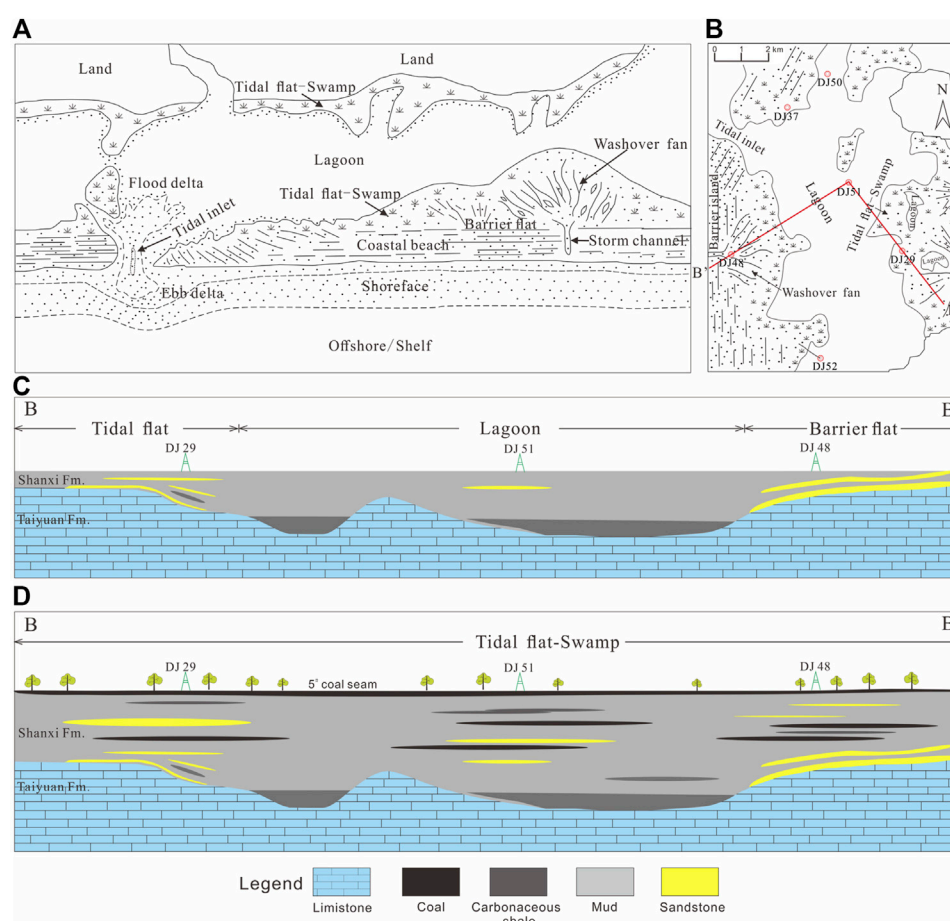


FIGURE 14

Comprehensive comparison of the barrier island-lagoon sedimentary model in the Shan-2 Lower Sub-member in the eastern Ordos Basin. (A) Plane of the barrier coast sedimentary model (according to P.A. Scholle and D. Spearing, 1982; as quoted and modified from Sun and Li, 1986). (B) Plane of the barrier island-lagoon sedimentary model in the study area. Profiles of the barrier island-lagoon sedimentary model during the early stage (C) and the later stage (D) of the Shan-2 Lower Sub-member.

studying the lithofacies combination, sedimentary structure, geochemical parameters, and paleontology, considered the Shan-2 Member to be primarily a lagoon sedimentary environment with weak hydrodynamic conditions and a weak-reduction water body. They proposed that the Shan-2 Member in the Daning-Jixian area is a typical barrier island-lagoon sedimentary model. Zhang et al. (2021) considered the shale in the lower part of the Shanxi Formation to have high TOC, Sr/Ba, and U/Th, formed in a lagoon sedimentary environment. The lower part of the Shanxi Formation is composed of barrier island facies, lagoon facies, delta front facies, and swamp facies. Through core observation and geochemical element characteristics analysis, Gu et al. (2022) considered Section 1 of the Shan-2 Lower sub-member to be dominated by marine bay facies. Starting from the deposition of Section 2, the frequent changes of water lead to changes in sedimentary facies, with the upper section principally

composed of transitional facies such as lagoon, tidal flat, and swamp facies.

Against a regional sedimentary background, based on the lithologic spatial distribution characteristics of each section in the Shan-2 Lower Sub-member in the study area, combined with the paleogeomorphology, seismic facies, and indicator characteristics of the sedimentary environment, there may be two sedimentary models suitable for this area. One is the barrier island-lagoon sedimentary model, which mainly develops the barrier island-tidal flat-lagoon sedimentary combination (Figure 14A). This model applies to the landward side of barrier terrains such as sand bars and uplifts, which are only connected to the open sea by a tidal inlet, and where the circulation of nearshore seawater is blocked, forming a barrier island-lagoon sedimentary system. Hydrodynamic energy is low and the seawater can be saline or desalinated (Chen et al., 2004; Zhu, 2008).

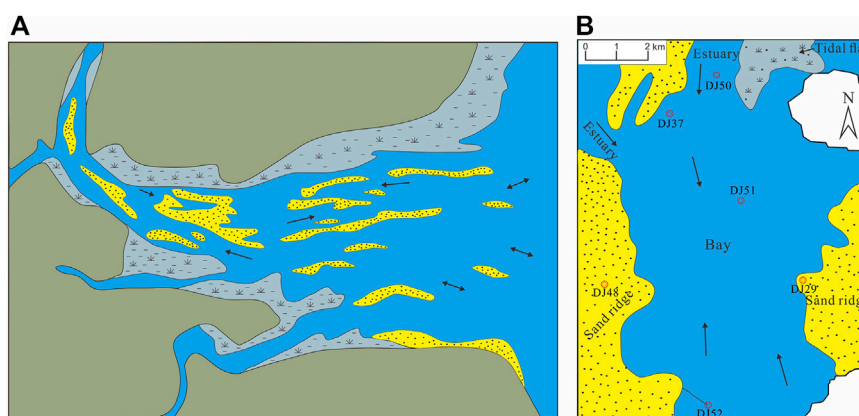


FIGURE 15

Comprehensive comparison of the estuarine sedimentary model in the Shan-2 Lower Sub-member in the eastern Ordos Basin. (A) Plane of the estuarine sedimentary model (according to M.O. Hayes, 1976; as quoted and modified from Sun and Li, 1986). (B) Plane of the estuarine sedimentary model in the study area.

The other model is an estuarine sedimentary model, in which estuarine facies and tidal flat facies are developed. The estuarine sedimentary model is mainly influenced by the dual effects of rivers and tides, and the system is formed in transgressive periods. It is connected with the broad sea on the outside, exhibiting a contour which widens seaward (Figure 15A). Estuaries are usually semi-closed coastal water bodies diluted by rivers (Chen et al., 2004; Li et al., 2018).

5.4.1 Barrier island-lagoon sedimentary model

In the early depositional period of the Shan-2 Lower Sub-member (Sections 1 and 2), the area of Wells DJ48-DJ37 and the eastern area of Well DJ29 are in a high landform, which has the geomorphic conditions for forming barrier islands. The sedimentary environment is dominated by high energy and the hydrodynamic force is relatively strong, with the lithology mainly sandstone deposition. The low geomorphic area is located in the middle of the study area, its water body is relatively deep, and its energy is relatively weak. It represents a sub-high-energy, weak reduction environment, with a lithology dominated by gray-black and carbonaceous shale. At the later stage of deposition of the Shan-2 Lower Sub-member (Sections 3 and 4), the landform fluctuation was weakened, the water became shallow, and the water body changed frequently under tidal action. It is mainly in a shallow-water, weak oxidation transitional environment, and the lithology is dominated by a complex interbedding of fine-grained sandstone, silty shale, shale, carbonaceous shale, and coal seam.

The results indicate that a barrier island-lagoon sedimentary model is developed in the study area (Figure 14B). In the early stage of the Shan-2 Lower Sub-member, there is a barrier island-lagoon-tidal flat sedimentary combination. The barrier islands are developed on both sides of the study area, and barrier flat

deposits with high landform are mainly developed in the area of Wells DJ48-DJ37 and to the east of Well DJ29, providing conditions for the formation of closed and semi-closed lagoons. The tidal inlet may be located south-west of Well DJ37 or north-east of the study area. Low geomorphic areas such as Well DJ51 are dominated by lagoon facies, mainly gray-black shale and silty shale deposition under anoxic (weak reduction) water conditions, which was a favorable facies belt for the deposition of organic-rich shale; it is also a key target section for transitional facies shale gas exploration in this area. The profile of its sedimentary model is shown in Figure 14C.

During the later stage, the Shan-2 Lower Sub-member was weakened by geomorphic control, forming a shallow-water, high-energy, weak oxidation transitional environment. At this time, because of the warm and humid climate and the influx of debris flow (Zhang et al., 2021; Gu et al., 2022), the sedimentary environment of the low geomorphic area changed from lagoon to tidal flat facies. Moreover, many sets of thin coal seams are developed down-hole. Therefore, it is considered that the Shan-2 Lower Sub-member evolved into a tidal flat-swamp sedimentary environment; its sedimentary model profile is shown in Figure 14D.

5.4.2 Estuarine sedimentary model

The Shan-2 Lower Sub-member is dominated by a high-energy and sub-high-energy, transitional environment, with a relatively strong hydrodynamic force. In the early stage of the Shan-2 Lower Sub-member (Sections 1 and 2), the down-hole lithology of Wells DJ48, DJ37, and DJ29 were mostly sandy sediment. Shale was often intercalated between sand layers, with the particle size becoming gradually finer as one moves upward. In addition, there are high geomorphic characteristics near well DJ48. The sand body is

relatively developed and its distribution scale is large: the thickness of the sand body is 8–10 m, the width can reach 1,500–2000 m, and the length is ~8 km. The area to the east of well DJ29 is also dominated by sandstone deposition; the landform is relatively high, the sand body is 6–7 m thick, 2000 m wide, and 5 km long. The landform in the middle of the study area is low, the sedimentary water is relatively deep, and energy is weak. It is mainly a sub-high-energy, weak reduction transitional environment, composed of fine-grained sediments such as dark shale and gray–black carbonaceous shale. At the later stage of the Shan-2 Lower Sub-member (Sections 3 and 4), the landform fluctuation was relatively gentle and the water was shallow. The sedimentary environment is a shallow-water, high-energy, weak oxidation transitional environment, its lithology dominated by shale and carbonaceous shale, with locally deposited sandstone and coal seams.

The analysis indicates that the Shan-2 Lower Sub-member in the study area fits an estuarine sedimentary model (Figure 15B). The early stage of the Shan-2 Lower Sub-member is a tidal-dominant estuarine sedimentary environment. The area of Well DJ48, to the north of Well DJ37, and to the east of Well DJ29 are sand ridges formed under an estuarine environment. The estuary may be located near Well DJ50 and southwest of Well DJ37. The low geomorphic area of Well DJ51 in the middle of the study area is mainly marine bay facies.

In the later stage of deposition, primarily in a shallow-water, high-energy, weak oxidation transitional environment, the down-hole lithology is interbedded with shale and silty shale, and the thin coal seams were increased, indicating frequent sea level changes at this time. Based on the coal seam formation environment and the lithologic spatial characteristics, this period gradually seems to have evolved into a tidal flat-swamp facies sedimentary environment.

5.4.3 Discussion of the sedimentary model

Comparison of the sedimentary characteristics of the two types of sedimentary models above indicates that the lagoon facies sediments in the barrier island-lagoon sedimentary model are mostly silt and mud and mainly developed horizontal bedding which comprised monotonic biological species with small bodies and thin shells; the overall scale of the barrier island is relatively large. However, complex and diverse sedimentary structures are often developed in estuarine sediments, and bioturbation structures are relatively developed. Biological burrows and host structures are more common in argillaceous sediments. There are abundant types of biological fossils and the individual organisms change from land to sea. The sedimentary range of the estuarine system has certain limitations and the scale of the sand ridge is relatively small (Chen et al., 2004; Zhu, 2008; Jiang, 2010; Boggs, 2012).

Based on the actual sedimentary characteristics of the study area, the geomorphological pattern lays a foundation for the formation of a sedimentary system. In the early stage of the Shan-2 Lower Sub-member, the low geomorphic area in the middle of the study area was mainly composed of dark shale and shales, and was characterized by horizontal bedding. The type of biological debris at the bottom of the

Shan-2 Lower Sub-member was relatively simple, consisting mainly of small crinoids and brachiopods. Sections 1 and 2 have high TOC content, high Sr/Ba, Ni/Co, U/Th, Sr/Cu ratio, and low Ti, Zr, and Al content (Dong et al., 2021; Wu et al., 2021; Gu et al., 2022; Sun et al., 2022), reflecting lower energy, brackish, and weak-reduction water, which indicate a lagoon sedimentary environment. The sandy sediment deposition scale in the high geomorphic area was relatively large, being more consistent with the sedimentary characteristics of barrier island facies. In the later stage of the Shan-2 Lower Sub-member, the landform fluctuation was relatively gentle, the increasing contents of Ti, Zr, and Al, and low Sr/Cu, Sr/Ba, Ni/Co, and U/Th (Gu et al., 2022) reflecting a shallow-water, high-energy, weak oxidation transitional environment. The down-hole lithology was mainly gray silty shale, carbonaceous shale, and thin coal seams, the lithology changed frequently in the vertical direction, and plant stump fossils can be seen in the shale, indicating that tidal flat-swamp facies dominated at this time.

6 Conclusion

- 1) The lithology distribution of transitional shale strata in the Shan-2 Lower Sub-member is significantly different, with complex and diverse lithologic combinations. The geomorphological pattern of interjacent depressions and highlands lays a foundation for the formation of a sedimentary system, and the environmental and energy differences of paleo-sedimentary water form a sedimentary environment with frequent facies transitions, controlling the distribution of sediments.
- 2) The early stage of deposition shows that the geomorphic uplift area was characterized by a high-energy transitional environment, mainly with developed sandstone and silty mudstone. The depression was a relatively low energy, brackish water reduction environment, mainly composed of dark and carbonaceous shales. In the later stage of deposition, the geomorphic control weakened, thus presenting a shallow water, high-energy, and oxidized transitional environment. The lithology was dominated by the complex interbedding of fine-grained sandstone, silty shale, shale, carbonaceous shale, and coal seam.
- 3) The spatial distribution of lithology, the changes in landform, and the shale sedimentary environment indicate that the Shan-2 lower sub-member developed a typical barrier island-lagoon sedimentary model. The early depositional period was dominated by barrier island-lagoon-tidal flat depositional assemblages. The barrier island was formed in the high landform area on both sides of the study area, and the low landform area was dominated by the lagoon facies, which was the favorable facies belt for the deposition of organic-rich shale. At the later stage of deposition, the sedimentary environment gradually evolved into a tidal flat-swamp environment. During this period, the sea level decreased, the terrigenous debris inflow increased,

and the paleo-redox environment tended to be oxic, which was not conducive to the preservation of shale organic matter.

Data availability statement

The original contributions presented in the study are included in the article/Supplementary Material, and further inquiries can be directed to the corresponding author.

Author contributions

LZ: conceptualization, funding acquisition, validation, supervision. XW: data curation, methodology, writing—original draft preparation. YW: project administration, software and methodology. SL, YG, and XL: investigation, resources. All authors contributed to the article and approved the submitted version.

Funding

This study was supported by the Science and Technology Cooperation Project of the CNPC-SWPU Innovation Alliance (Grant No. 2020CX030103).

References

- Boggs, S., Jr. (2012). *Principles of sedimentology and stratigraphy [M]*. 5th ed. Boston: Pearson India.
- Boyd, R., Dalrymple, R., and Zaitlin, B. A. (1992). Classification of clastic coastal depositional environments. *Sediment. Geol.* 80 (3/4), 139–150. doi:10.1016/0037-0738(92)90037-R
- Chen, J. Q., Zhou, H. R., and Wang, X. L. (2004). *A course in sedimentology and paleogeography[M]*. Beijing: Geological Publishing House, 131–133.
- Chen, L., Lu, Y., Jiang, S., Guo, T., and Luo, C. (2015). Heterogeneity of the lower silurian longmaxi marine shale in the southeast sichuan basin of China. *Mar. Petroleum Geol.* 65, 232–246. doi:10.1016/j.marpetgeo.2015.04.003
- Ding, C. Q., Zhou, L., Zhong, K. X., Wu, Y., Zhong, F. Y., and Liu, Y. (2020). Prediction of changxing formation reef reservoir in damaoping area, eastern sichuan[J]. *Xinjiang Pet. Geol.* 41 (02), 164–171. doi:10.7657/XJPG20200205
- Dong, D. Z., Qiu, Z., Zhang, L. F., Li, S. X., Zhang, Q., Li, X. T., et al. (2021). Research progress and new discovery of shale gas strata in marine-continent transitional facies shale gas[J]. *Acta Sedimentol. Sin.* 39 (01), 29–45. doi:10.14027/j.issn.1000-0550.2021.002
- Dong, D. Z., Wang, Y. M., Li, X. J., Zou, C. N., Guan, Q. Z., Zhang, C. C., et al. (2016). Breakthrough and prospect of shale gas exploration and development in China[J]. *Nat. Gas. Ind.* 36 (01), 19–32. doi:10.3787/j.issn.1000-0976.2016.01.003
- Dong, D. Z., Zou, C. N., Yang, H., Wang, Y. M., Li, X. J., Chen, G. S., et al. (2012). Progress and prospects of shale gas exploration and development in China[J]. *Acta Pet. Sin.* 33 (S1), 107–114.
- Feng, W. M., Xie, Y., Liu, J. Q., Lin, J. H., Chen, G., and Zhao, Z. (2016). Sedimentological significance of marine carbonate natural gamma-ray spectroscopy logging data-taking the Cambrian Qingxudong Formation in L1 well of southeast Sichuan as an example [J]. *Mar. Geol. Quat. Geol.* 36 (05), 165–172. doi:10.16562/j.cnki.0256-1492.2016.05.017
- Galloway, W. E. (1998). Clastic depositional systems and sequences: Applications to reservoir prediction, delineation, and characterization. *Lead. Edge* 17 (2), 173–180. doi:10.1190/1.1437934
- Gu, Y. F., Li, X. T., Li, S. X., Jiang, Y. Q., Fu, Y. H., Yang, X. S., et al. (2022). Sedimentology and geochemistry of the lower permian Shanxi Formation Shan23 sub-member transitional shale, eastern Ordos Basin, NorthChina. *Front. Earth Sci. (Lausanne)*. 10, 859845. doi:10.3389/feart.2022.859845
- Guan, Q. Z., Dong, D. Z., Zhang, H. L., Sun, S. S., Zhang, S. R., and Guo, W. (2021). Types of biogenic quartz and its coupling storage mechanism in organic-rich shales: A case study of the upper ordovician wufeng formation to lower silurian longmaxi Formation in the sichuan basin, SW China. *Petroleum Explor. Dev.* 48 (4), 813–823. doi:10.1016/S1876-3804(21)60068-X
- Guo, X. S., Hu, D. F., Liu, R. B., Wei, X. F., and Wei, F. B. (2018). Geological conditions and exploration potential of Permian marine continental transitional facies shale gas in Sichuan Basin. *Nat. Gas. Ind.* 38 (10), 11–18. doi:10.3787/j.issn.1000-0976.2018.10.002
- He, S., Qin, Q. R., Fan, C. H., Zhou, J. L., Zhong, C., and Huang, W. (2019). Shale reservoir characteristics and influencing factors of wufeng-longmaxi Formation in dingshan area, southeast sichuan[J]. *Petroleum Reserv. Eval. Dev.* 9 (04), 61–67+78. doi:10.13809/j.cnki.cn32-1825/te.2019.04.012
- Hou, G. F., Qu, J. H., Zhu, F., Xu, Y., Sun, J., Wang, L. B., et al. (2018). Controlling effect of paleogeomorphology on sedimentary system and sedimentary microfacies – a case study of Cretaceous Qingshuihe Formation in the hinterland of Junggar Basin[J]. *J. China Univ. Min. Technol.* 47 (05), 1038–1045. doi:10.13247/j.cnki.jcmt.000829
- Jiang, Q. C., Wang, H., Li, D., Cao, F., Li, Q. F., Sun, Z. X., et al. (2012). Application conditions of seismic waveform classification technology and its application in the study of sedimentary microfacies in the northern region of Pubei[J]. *Oil gas Geol.* 33 (01), 135–140.
- Jiang, Z. X. (2010). *Sedimentology [M]*. 2nd ed. Beijing: Petroleum Industry Press.
- Jin, M. D., Tan, X. C., Tong, M. S., Zeng, W., Liu, H., Zhong, B., et al. (2017). Karst paleogeomorphology of the fourth member of sinian dengying Formation in gaoshiti-moxi area, sichuan basin, SW China: Restoration and geological significance. *Petroleum Explor. Dev.* 44 (1), 58–68. doi:10.1016/s1876-3804(17)30008-3

Acknowledgments

The authors sincerely thank PetroChina Coalbed Methane Company Limited for providing the cores and seismic data for this study.

Conflict of interest

SL and XL were employed by PetroChina Coalbed Methane Company.

The remaining authors declare that the research was conducted in the absence of any commercial or financial relationships that could be construed as a potential conflict of interest.

Publisher's note

All claims expressed in this article are solely those of the authors and do not necessarily represent those of their affiliated organizations, or those of the publisher, the editors and the reviewers. Any product that may be evaluated in this article, or claim that may be made by its manufacturer, is not guaranteed or endorsed by the publisher.

- Konitzer, S. F., Davies, S. J., Stephenson, M. H., and Leng, M. J. (2014). Depositional controls on mudstone lithofacies in a basin setting: Implications for the delivery of sedimentary organic matter. *J. Sediment. Res.* 84 (3), 198–214. doi:10.2110/jsr.2014.18
- Kuang, L. C., Dong, D. Z., He, W. Y., Wen, S. L., Sun, S. S., Li, S. X., et al. (2020). Geological characteristics and exploration of shale gas in the transitional facies of the eastern margin of Ordos Basin Development prospects[J]. *Petroleum Explor. Dev.* 47 (03), 435–446. doi:10.11698/PED.2020.03.01
- Li, S. L., Xu, L., Yu, X. H., Hou, G. W., Hu, Y., and Gao, Z. P. (2018). Oligocene transgression and sedimentary characteristics of tidal control system in xihu sag, east China sea shelf basin. *J. Palaeogeogr.* 20 (06), 1023–1032. doi:10.7605/gdxb.2018.06.075
- Li, W. H., Zhang, Q., Li, K. Y., Chen, Q., Guo, Y. Q., Ma, Y., et al. (2021). The late paleozoic sedimentary evolution in the Ordos Basin and its peripheral areas[J]. *J. Palaeogeogr.* 23 (01), 39–52. doi:10.7605/gdxb.2021.01.003
- Liang, Q. S., Zhang, X., Tian, J. C., Sun, X., and Chang, H. L. (2018a). Geological and geochemical characteristics of marine-continental transitional shale from the lower permian Taiyuan Formation, taikang uplift, southern north China basin. *Mar. Petroleum Geol.* 98, 229–242. doi:10.1016/j.marpetgeo.2018.08.027
- Liang, X. T., Zhang, Y. R., and Zhang, H. Q. (2018b). Characteristics of gamma energy spectrum, sedimentary environment and comprehensive evaluation of shale reservoirs in Western Hubei[J]. *Resour. Environ. Eng.* 32 (04), 576–583+589. doi:10.16536/j.cnki.issn.1671-1211.2018.04.011
- Liu, J. Y., Steel, R. J., Lin, C. S., Yang, H. J., Yang, Y. H., Peng, L., et al. (2012). Geomorphology control on the development of reservoir depositional systems, devonian donghetang Formation in the tabei uplift of the tarim basin, China. *Mar. Petroleum Geol.* 38 (1), 177–194. doi:10.1016/j.marpetgeo.2012.06.009
- Liu, S. X., Wu, C. F., Li, T., and Wang, H. C. (2018). Multiple geochemical proxies controlling the organic matter accumulation of the marine-continental transitional shale: A case study of the upper permian longtan formation, Western guizhou, China. *J. Nat. Gas Sci. Eng.* 56, 152–165. doi:10.1016/j.jngse.2018.06.007
- Lu, J. M., and Wang, Y. G. (2009). *Principles of seismic exploration[M]*. Dongying: China University of Petroleum Press, 371–380.
- Luo, H. H. (2013). *Evaluation and fine characterization of mud shale reservoir in marine and land interaction[D]*. Beijing: China University of Geosciences.
- Luo, W., Hou, M. C., Liu, X. C., Huang, S. G., Chao, H., Zhang, R., et al. (2018). Geological and geochemical characteristics of marine-continental transitional shale from the Upper Permian Longtan formation, Northwestern Guizhou, China. *Mar. Petroleum Geol.* 89, 58–67. doi:10.1016/j.marpetgeo.2017.06.029
- Meng, Q. A., and Ji, Y. L. (2009). Controlling effect of Cretaceous paleogeomorphology on the distribution of sedimentary systems in Tanan Depression[J]. *Acta Pet. Sin.* 30 (06), 843–848+855.
- Qiu, Z., Song, D. J., Zhang, L. F., Zhang, Q., Zhao, Q., Wang, Y. M., et al. (2021). The geochemical and pore characteristics of a typical marine-continental transitional gas shale: A case study of the permian Shanxi Formation on the eastern margin of the Ordos Basin. *Energy Rep.* 7, 3726–3736. doi:10.1016/j.egyr.2021.06.056
- Qiu, Z., and Zou, C. N. (2020). Controlling factors on the formation and distribution of "Sweet-Spot areas" of marine gas shales in south China and a preliminary discussion on unconventional Petroleum sedimentology. *J. Asian Earth Sci.* 194, 103989. doi:10.1016/j.jseas.2019.103989
- Sheriff, R. E. (1982). *Structural interpretation of seismic data[M]*. Tulsa: American Association of Petroleum Geologists.
- Sun, Y. C., and Li, H. S. (1986). *Sedimentary facies and sedimentary environment of clastic rocks*. Beijing: Geological Publishing House.
- Sun, Y., Jiang, Y. Q., Xiong, X. Y., Li, X. T., Li, S. X., Qiu, Z., et al. (2022). Lithofacies and sedimentary environment evolution of transitional shale in Shanxi Formation Shan23 sub-member, daning-jixian area, eastern Ordos Basin [J/OL]. *Coal Geol. Explor.* 1-12. [2022-07-19]. doi:10.12363/issn.1001-1986.21.12.0821
- Sun, Z. P., Wang, Y. L., Wei, Z. F., Zhang, M. F., Wang, G., and Wang, Z. X. (2017). Characteristics and origin of desorption gas of the permian Shanxi Formation shale in the Ordos Basin, China. *Energy Explor. Exploitation* 35 (6), 792–806. doi:10.1177/0144598717723564
- Tian, W. (2016). *Research on the permian Shanxi Formation sedimentary system in the southeast of Ordos Basin[D]*. Xi'an: Northwest University.
- Ursula, H., and Gregory, F. (2012). Haynesville and bossier mudrocks: A facies and sequence stratigraphic investigation, east Texas and Louisiana, USA. *Mar. Pet. Geol.* 31 (1), 8–26. doi:10.1016/j.marpetgeo.2011.10.001
- Wang, S. J., Li, D. H., Li, J. Z., Dong, D. Z., Zhang, W. Z., and Ma, J. (2011). Exploration potential of shale gas in the Ordos Basin. *Nat. Gas. Ind.* 31 (12), 40–46. doi:10.3787/j.issn.1000-0976.2011.12.006
- Wei, Z. F., Wang, G., Wang, Y. L., Ma, X. Y., Zhang, T., He, W., et al. (2020). Geochemical and geological characterization of marine-continental transitional shale: A case study in the Ordos Basin, NW China. *Acta Geol. sinica- Engl. Ed.* 94 (3), 809–821. doi:10.1111/1755-6724.13888
- Wu, J., Wang, H. Y., Shi, Z. S., Wang, Q., Zhao, Q., Dong, D. Z., et al. (2021). Predominant lithofacies types and genetic mechanism of black shale of marine-terrestrial transition facies: Taking the Permian Shanxi Formation in the eastern margin of the Ordos Basin Take as an example[J]. *Petroleum Explor. Dev.* 48 (06), 1137–1149. doi:10.11698/PED.2021.06.06
- Xiao, H., Wang, T. G., Li, M. J., Lai, H. F., Liu, J. G., Mao, F. J., et al. (2019). Geochemical characteristics of Cretaceous Yogou Formation source rocks and oil-source correlation within a sequence stratigraphic framework in the Termit Basin, Niger. *J. Petroleum Sci. Eng.* 172, 360–372. doi:10.1016/j.petrol.2018.09.082
- Xu, G. Q., and Haq, B. U. (2022). Seismic facies analysis: Past, present and future. *Earth-Science Rev.* 224, 103876. doi:10.1016/j.earscirev.2021.103876
- Yan, D. Y., Huang, W. H., Li, A., Liu, H., and Liu, H. L. (2013). Preliminary analysis of marine-continental transitional shale gas accumulation conditions and favorable areas in the Upper Paleozoic Ordos basin[J]. *J. Northeast Petroleum Univ.* 37 (05), 1–9. doi:10.3969/j.issn.2095-4107.2013.05.001
- Yang, Y. T., Li, W., and Ma, L. (2005). Tectonic and stratigraphic controls of hydrocarbon systems in the Ordos Basin: A multicycle cratonic Basin in central China. *Am. Assoc. Pet. Geol. Bull.* 89, 255–269. doi:10.1306/10070404027
- Zhang, L. F., Dong, D. Z., Qiu, Z., Wu, C. J., Zhang, Q., Wang, Y. M., et al. (2021). Sedimentology and geochemistry of Carboniferous-Permian marine-continental transitional shales in the eastern Ordos Basin, North China. *Palaeogeogr. Palaeoclimatol. Palaeoecol.* 571 (1–3), 110389. doi:10.1016/j.palaeo.2021.110389
- Zhang, P. (2015). *The control effect and application of sedimentary environment on shale gas development[D]*. Beijing: China University of Geosciences.
- Zhang, Q., Qiu, Z., Zhang, L. F., Wang, Y. M., Xiao, Y. F., Liu, D., et al. (2022). Reservoir characteristics and its influence on transitional shale: An example from Permian Shanxi Formation shale, Daning-Jixian blocks, Ordos Basin[J]. *Nat. Gas. Geosci.* 33 (3), 396–407. doi:10.11764/j.issn.1672-1926.2021.07.002
- Zhang, S. H., Liu, C. Y., Liang, H., Wang, J. Q., Bai, J. K., Yang, M. H., et al. (2018). Paleoenvironmental conditions, organic matter accumulation, and unconventional hydrocarbon potential for the Permian Lucaogou Formation organic-rich rocks in Santanghu Basin, NW China. *Int. J. Coal Geol.* 185, 44–60. doi:10.1016/j.coal.2017.11.012
- Zhao, J. H., Jin, Z. J., Jin, Z. K., Wen, X., Gen, Y. K., Yan, C. N., et al. (2016). Lithofacies types and sedimentary environment of shale in wufeng-longmaxi formation, sichuan basin[J]. *Acta Pet. Sin.* 37 (05), 572–586. doi:10.7623/syxb201605002
- Zhu, G. Y., Jin, Q., Zhang, S. C., and Zhang, L. Y. (2003). Forming mechanisms and heterogeneity of source rock: A case study in dongying depression. *Mineralogy Petrology* 23 (4), 95–100. doi:10.19719/j.cnki.1001-6872.2003.04.022
- Zhu, X. M. (2008). *Sedimentary petrology [M]*. 4th ed. Beijing: Petroleum Industry Press.
- Zou, C. N., Dong, D. Z., Wang, Y. M., Li, X. J., Huang, J. L., Wang, S. F., et al. (2015). Shale gas in China: Characteristics, challenges and prospects (I). *Petroleum Explor. Dev.* 42 (6), 753–767. doi:10.1016/S1876-3804(15)30072-0
- Zou, C. N., Dong, D. Z., Wang, Y. M., Li, X. J., Huang, J. L., Wang, S. F., et al. (2016). Shale gas in China: Characteristics, challenges and prospects(II)[J]. *Petroleum Explor. Dev.* 43 (02), 166–178. doi:10.11698/PED.2016.02.02